E4-98-281

R.V.Jolos, A.K.Nasirov*, G.G.Adamian*, A.I.Muminov*

# EFFECT OF SHELL STRUCTURE ON ENERGY DISSIPATION IN HEAVY-ION COLLISIONS

Submitted to «Physical Review C»

*Heavy Ion Physics Department, Institute of Nuclear Physics 702132 Ulugbek, Tashkent, Uzbekistan

1998

# 1 Introduction

Dissipation of a large amount of the kinetic energy in deep inelastic heavy ion collisions (DIC) is a fundamental time-dependent process [1,2] that has attracted theoretical interest since the discovery of this class of reactions. At an earlier stage of investigations it was assumed that the excitation energy is distributed between reaction partners in proportion to their masses. However, after a series of experiments, it became clear that a large part of the excitation energy is concentrated in the light fragments for a wide range of total kinetic energy losses (TKEL). Various models have been proposed to explain this phenomena, taking into account a coupling of the relative motion to the intrinsic degrees of freedom. The simple macroscopic models with phenomenological friction forces can not be used to treat this problem. In microscopic models, friction forces are derived considering a coupling of the relative motion to the specific intrinsic degrees of freedom. However, not all of these models can consider a division of the excitation energy between the reaction partners.

To microscopic models, which can make predictions for the excitation energy partitioning between the reaction partners, belong the model developed in [3]. In this model, all transport phenomena are assumed to be mediated by the exchange of independent nucleons between interacting nuclei. Sufficient amounts of the kinetic energy is dissipated when large numbers of nucleons are transferred in alternating directions. Usually, in deep inelastic heavy ion collisions, a shift of the centroid of the mass distributions is small in comparison with the width. Therefore, it is expected that both nuclei receive, on the average, comparable amounts of excitation energy. In the model [3], which is based on the Fermi-gas model for the intrinsic motion, the kinetic energy losses are explained by the fact that the intrinsic momentum of a transferred nucleon is summed with the momentum of the relative motion. As a result, this momentum can be larger than the Fermi momentum $P_F$, thus producing the excitation of a donor nucleus.

For relative velocities of the interacting nuclei at which the adiabatic approximation loses its accuracy, the model developed in [4,5] suggests that particle–hole states are excited in the two interacting nuclei as a result of diabatic transitions between the single-particle levels of a time-dependent one-body potential. Thus, in this model, a description of the dissipative processes is strongly based on the single-particle level schemes in the two-center potential well of a dinuclear system. Detailed calculations based on this model for the $^{139}$La+$^{109}$Ag reaction [6] have shown that the excitation energy per nucleon $\epsilon^*$ is smaller for the heavier reaction partner. At the same time, it

is known from the calculations of inelastic processes in nucleus-nucleus collisions that appreciable energy dissipation takes place even before the first crossing of the single-particle levels near the Fermi surface [7]. Therefore, it is necessary to look for other possibilities to explain an observed partition of the excitation energy between reaction partners.

The important aspect of the description of a nucleon transfer and a kinetic energy dissipation is connected with an influence of the peculiarities of the shell structure of the interacting nuclei on the correlations between the kinetic energy loss and the width of the fragment charge distribution. Indeed, it was demonstrated in [1, 8-11] by analysing the experimental data for different reactions that these correlations are sensitive to the projectile-target combination.

So, it is interesting also to investigate the effect of the shell structure near the Fermi surface on the sharing of the excitation energy between fragments of binary reactions. This is the aim of the present paper.

In fact, we will investigate an influence of the single particle level density near the Fermi surface on these characteristics. The calculations are performed with the experimentally determined single-particle scheme of Ca isotopes and with the single-particle scheme in which the level density is doubled artificially. The proton and neutron separation energies remain constant. In [12-14], we developed a microscopic approach to describe the loss of the total kinetic energy and its partitioning between the reaction partners in DIC. Using this model, we have succesfully described different characteristics of deep inelastic reactions, such as the centroid positions and the width of the mass and charge distributions as functions of the excitation energy and partition of the excitation energy between the reaction product.

Comparing our model to the model [3], we should mention that in principle the effect of the addition of relative and intrinsic nucleon momenta can be taken into account. In order to do this it is necessary to transform the Hamiltonian into an intrinsic frame. Then, the additional terms depending on the velocity of the relative motion will appear in the Hamiltonian. These new terms will contribute to the matrix elements of the single nucleon transfer and, therefore, will influence the kinetic energy dissipation process. However, this effect is not included in the present calculations.

## 2 Model

It is convenient to start with the total Hamiltonian of a dinuclear system written in the form

$$\hat{H} = \hat{H}_{rel}(\mathbf{R};\mathbf{P}) + \hat{H}_{in}(\xi) + \delta\hat{V}(\mathbf{R},\xi), \tag{1}$$

where the Hamiltonian of a relative motion,

$$\hat{H}_{rel}(\mathbf{R};\mathbf{P}) = \frac{\hat{\mathbf{P}}^2}{2\mu} + \hat{\mathcal{V}}(\hat{\mathbf{R}}), \tag{2}$$

consists of the kinetic energy operator and the nucleus-nucleus interaction potential $\hat{\mathcal{V}}(\hat{\mathbf{R}})$. Here, $\hat{\mathbf{R}}$ is the relative distance between the centers of mass of the fragments, $\hat{\mathbf{P}}$ is the conjugate momentum, and $\mu$ is the reduced mass of the system; $\xi$ is a set of relevant intrinsic variables. The last two terms in (1) describe the internal motion of nuclei and the coupling between the relative and internal motions (for details, see [12,13]). It is clear that the coupling term leads to a dissipation of the kinetic energy into the energy of internal nucleon motion. Our further consideration will be concentrated on this term.

Let us take a sum of the last two terms in (1) as a single-particle Hamiltonian of a dinuclear system $\hat{\mathcal{H}}$ plus a residual interaction,

$$\begin{aligned} \hat{H}_{in}(\xi) + \delta\hat{V}(\mathbf{R},\xi) &= \hat{\mathcal{H}}(\mathbf{R}(t),\xi) + h_{residual}, \\ \hat{\mathcal{H}}(\mathbf{R}(t)) &= \sum_{i=1}^{A}\left(\frac{-\hbar^2}{2m}\Delta_i + \hat{V}_P(\mathbf{r}_i - \mathbf{R}(t)) + \hat{V}_T(\mathbf{r}_i)\right), \end{aligned} \tag{3}$$

where $m$ is the nucleon mass and $A = A_P + A_T$ is the total number of nucleons in the system.

Then, in the second quantization representation, the Hamiltonian $\hat{\mathcal{H}}(\mathbf{R}(t),\xi)$ can be written as

$$\hat{\mathcal{H}}(\mathbf{R}(t),\xi) = \sum_P \varepsilon_P \mathrm{a}_P^+\mathrm{a}_P + \sum_T \varepsilon_T \mathrm{a}_T^+\mathrm{a}_T + \sum_{i,i'} V_{ii'}(\mathbf{R}(t))\mathrm{a}_i^+\mathrm{a}_{i'}, \tag{4}$$

where

$$\sum_{i,i'} V_{ii'}(\mathbf{R}(t))\mathrm{a}_i^+\mathrm{a}_{i'} = \sum_{P,P'} \Lambda^{(T)}_{PP'}(\mathbf{R}(t))\mathrm{a}_P^+\mathrm{a}_{P'} + \sum_{T,T'} \Lambda^{(P)}_{TT'}(\mathbf{R}(t))\mathrm{a}_T^+\mathrm{a}_{T'} + (5)$$
$$\sum_{T,P} \mathrm{g}_{PT}(\mathbf{R}(t))(\mathrm{a}_P^+\mathrm{a}_T + \mathrm{H.c.}).$$

Here $P \equiv (n_P, j_P, l_P, m_P)$ and $T \equiv (n_T, j_T, l_T, m_T)$ are the sets of quantum numbers characterizing the single-particle state in an isolated projectile and target nuclei, respectively. The single-particle basis is constructed by the asymptotic wave vectors of the single-particle states of the noninteracting nuclei—the projectile ion $|P\rangle$ and the target nucleus $|T\rangle$—in the form

$$|\tilde{P}\rangle = |P\rangle - \frac{1}{2}\sum_T |T\rangle\langle T|P\rangle, \tag{6}$$

$$|\tilde{T}\rangle = |T\rangle - \frac{1}{2}\sum_P |P\rangle\langle P|T\rangle. \tag{7}$$

For this basis set, the orthogonality condition is satisfied up to terms linear in $\langle P|T\rangle$. Then

$$\Lambda^{(T)}_{PP'}(\mathbf{R}(t)) = \langle P|V_T(\mathbf{r})|P'\rangle, \tag{8}$$

$$\Lambda^{(P)}_{TT'}(\mathbf{R}(t)) = \langle T|V_P(\mathbf{r}-\mathbf{R}(t))|T'\rangle, \tag{9}$$

$$g_{PT}(\mathbf{R}(t)) = \frac{1}{2}\langle P|V_P(\mathbf{r}-\mathbf{R}(t)) + V_T(\mathbf{r})|T\rangle. \tag{10}$$

The nondiagonal matrix elements $\Lambda^{(T)}_{PP'}$ ($\Lambda^{(P)}_{TT'}$) generate the particle–hole excitations in the projectile (target) nucleus. The matrix elements $g_{PT}$ are responsible for the nucleon exchange between reaction partners. These matrix elements were calculated using the method proposed in [15, 16]. In (4), $\varepsilon_{P(T)}$ are the single-particle energies of the nonperturbed states in the projectile (target) nucleus. The coupling between the intrinsic nuclear degrees of freedom and the collective variable $\mathbf{R}$ is introduced by the $\mathbf{R}$ dependence of the sum of the single-particle potentials in (3). Since the trajectory calculation shows that the relative distance $\mathbf{R}(t)$ between the centers of the interacting nuclei could not be less than the sum of their radii, the tail of the partner single-particle potentials can be considered as a perturbation disturbing the asymptotic single-particle wave functions and their energies.

It is convenient to include the diagonal matrix elements of $V_{ii'}(\mathbf{R}(t))$ in $H_{in}$, introducing the renormalized $\mathbf{R}(t)$-dependent single-particle energies

$$\tilde{\varepsilon}_P(\mathbf{R}(t)) = \varepsilon_P + \langle P|V_T(\mathbf{r})|P\rangle, \tag{11}$$

$$\tilde{\varepsilon}_T(\mathbf{R}(t)) = \varepsilon_T + \langle T|V_P(\mathbf{r}-\mathbf{R}(t))|T\rangle. \tag{12}$$

Since explicit allowance for the residual interaction requires extensive calculations, it is customary to take the two-particle collision integral into account in linearized form ($\tau$-approximation).

To calculate the excitation energies of the reaction partners, we should find the occupation numbers of the single-particle states in both nuclei. They can be found by solving the equation for the single-particle density matrix $\tilde{n}$ in the form [12,13]

$$i\hbar\frac{\partial\hat{\tilde{n}}(t)}{\partial t} = [\hat{\mathcal{H}}(\mathbf{R}(t)),\hat{\tilde{n}}(t)] - \frac{i\hbar}{\tau}[\hat{\tilde{n}}(t) - \hat{\tilde{n}}^{eq}(\mathbf{R}(t))]\,, \tag{13}$$

where $\tilde{n}^{eq}(\mathbf{R}(t))$ is a local quasi-equilibrium distribution, *i.e.*, a Fermi distribution with the temperature $T(t)$ corresponding to the excitation energy at the internuclear distance $\mathbf{R}(t)$. Substituting our Hamiltonian (4) into (13), we get

$$\begin{aligned} i\hbar\frac{\partial\tilde{n}_i(t)}{\partial t} &= \sum_k [V_{ik}(\mathbf{R}(t))\tilde{n}_{ki}(t) - V_{ki}(\mathbf{R}(t))\tilde{n}_{ik}(t)] \\ &- \frac{i\hbar}{\tau_i}\left[\tilde{n}_i(t) - \tilde{n}_i^{eq}(t)\right], \end{aligned} \tag{14}$$

where $\tilde{n}_i$ is a diagonal and $\tilde{n}_{ik}$ is a nondiagonal matrix element of the density matrix. The approximate equation for nondiagonal matrix elements takes the form

$$\begin{aligned} i\hbar\frac{\partial\tilde{n}_{ik}(t)}{\partial t} &= \hbar\left[\tilde{\omega}_{ik}(\mathbf{R}(t)) - \frac{2i}{\tau_{ik}}\right]\tilde{n}_{ik}(t) \\ &+ V_{ki}(\mathbf{R}(t))\left[\tilde{n}_k(t) - \tilde{n}_i(t)\right], \end{aligned} \tag{15}$$

where we have used the notations $\tilde{\omega}_{ik} = [\tilde{\varepsilon}_i - \tilde{\varepsilon}_k]/\hbar$.

Substituting the solution of the Eq. (15) into Eq. (14), we get

$$\begin{aligned} \tilde{n}_i(\bar{t}) =& \exp\left(\frac{t-\bar{t}}{\tau_i}\right)\left\{\tilde{n}_i(t) + \frac{1}{\tau_i}\int_t^{\bar{t}} dt'\tilde{n}_i^{eq}(\mathbf{R}(t'))\exp\left(\frac{t'-t}{\tau_i}\right)\right. \\ &\left. + \sum_k \int_t^{\bar{t}} dt' \int_t^{t'} dt''\Omega_{ik}(t',t'')\exp\left(\frac{t''-\bar{t}}{\tau_{ik}}\right)\left[\tilde{n}_k(t'') - \tilde{n}_i(t'')\right]\right\}, \end{aligned} \tag{16}$$

where

$$\Omega_{ik}(t,t') = \frac{2}{\hbar^2}\mathrm{Re}\left\{V_{ik}(\mathbf{R}(t))V_{ki}(\mathbf{R}(t'))\exp\left[i\int_{t'}^{t} dt''\tilde{\omega}_{ki}(\mathbf{R}(t''))\right]\right\}. \tag{17}$$

The formal solution of Eq. (16) is found by dividing the interval $\bar{t} - t$ into small steps $\Delta t$. The time step $\Delta t$ used in the calculations is $0.8 \cdot 10^{-22}$ s which thus characterizes the time interval during which the **R**-dependent mean field of the combined dinuclear system changes so little that we can neglect the effect of this changing on the intrinsic motion. The results is

$$\tilde{n}_i(t+\Delta t) = \tilde{n}_i^{eq}(\mathbf{R}(t+\Delta t))\left[1 - \exp\left(\frac{-\Delta t}{\tau_i}\right)\right] + n_i(t+\Delta t)\exp\left(\frac{-\Delta t}{\tau_i}\right), \quad (18)$$

where

$$n_i(t+\Delta t) = \tilde{n}_i(t) + \sum_k \int_t^{t+\Delta t} dt' \Omega_{ik}(t',t') \frac{\sin[\tilde{\omega}_{ki}(\mathbf{R}(t'))(t'-t)]}{\tilde{\omega}_{ki}(\mathbf{R}(t'))} [\tilde{n}_k(t') - \tilde{n}_i(t')]. \quad (19)$$

Note that Eqs. (18) and (19) present an integral equation for $\tilde{n}_i(t)$.

One of our aims is to calculate the ratio of the excitation energies of the projectile-like ($E_P^*$) and target-like ($E_T^*$) fragments

$$R_{P/T} = E_P^*/E_T^*. \quad (20)$$

The excitation energies $E_{P(T)}^*$ are calculated step by step along the time scale using the equation

$$E_{P(T)}^*(t+\Delta t) = E_{P(T)}^*(t) + \sum_{P(T)} [\tilde{\varepsilon}_{P(T)}(\mathbf{R}(t)) - \lambda_{P(T)}(\mathbf{R}(t))][\tilde{n}_{P(T)}(t+\Delta t) - \tilde{n}_{P(T)}(t)]. \quad (21)$$

Total kinetic energy losses are defined as

$$E_{loss} = E_P^* + E_T^*. \quad (22)$$

As can be seen from Eqs. (16) and (17), the occupation numbers depend on an interaction matrix element $V_{ik}(\mathbf{R}(t))$, which is a short notation for $\chi_{PP'}^{(T)}$, $\chi_{TT'}^{(P)}$ describing particle-hole excitations in projectile-like and target-like nuclei, or $g_{PT}$, which is responsible for nucleon transfer. Thus, we can separately analyse the contribution of the two mechanisms—particle-hole excitations and the nucleon transfer—to the kinetic energy dissipation.

The variances $\sigma_Z^2$ and $\sigma_N^2$ are determined by occupation numbers through the equation

$$\sigma_{Z(N)}^2(t) = \sum_P^{Z(N)} \tilde{n}_P(t)[1 - \tilde{n}_P(t)]. \quad (23)$$

# 3 Results and discussion

The well-known nonequilibrium sharing of the excitation energy between fragments of the deep inelastic collisions was reviewed in [2]. The light and heavy products of deep inelastic heavy ion collisions are distinguished by the average energy distance between the single particle levels near the Fermi surface: in a light fragment, this energy distance is larger than in a heavy one. For this reason, on the average, the energy of the particle–hole excitation in a light fragment is larger than in a heavy fragment. Due to this fact, it is natural to assume that the main reason for a larger excitation energy per nucleon in a light fragment is the larger energy interval between the single-particle states in the light nucleus near the Fermi surface. Below, we will check this assumption. In fact, to establish the influence of the shell structure near the Fermi surface on nucleon transfer and the sharing of an excitation energy between the fragments of binary reactions, we will compare the results of calculations performed with the single-particle level scheme of a light nucleus that are well-established experimentally with those schemes which have an increased or decreased energy intervals compared to the experimental ones. Since the nucleon separation energy remains to be fixed, we can talk about variation of the single-particle level density near the Fermi surface.

As an example, consider the $^{40,48}$Ca $+^{248}$Cm reactions. The calculations are performed with the experimentally determined single-particle scheme of Ca isotopes and with the single-particle scheme in which the level density is doubled artificially. The proton and neutron separation energies remain constant. The results of the calculations are shown in Figs. 1a and 2a. It can be seen that $R^{P/T}$ decreases with the increase in the single-particle level density near the Fermi surfaces of the projectiles at the given TKEL, $E_{loss}$. The results of calculations for other combinations of the interacting nuclei confirm this tendency. The grounds for characterizing the interacting nuclei in deep inelastic heavy ion collisions by asymptotic single-particle level densities came from the fact that the interaction time is not large enough to reach complete equilibriation in dinuclear system before its decay. Thus, we can conclude that a larger value of the excitation energy per nucleon in the light fragment is explained by its lower single-particle level density near the Fermi surface compared to a heavy fragment.

In Figs. 1b and 2b, we show the results of calculations of the charge variance $\sigma_Z^2$ as a function of the total kinetic energy losses performed with different single-particle schemes for a light fragment. It can be seen that $\sigma_Z^2$ increases more rapidly with increasing of excitation energy if a single-particle

level density of the PLF takes a larger value. This result is in a correspondence with the experimentally observed influence of the shell structure on the correlation between the charge variance and TKEL [9, 11]. It was observed that TKEL increase more rapidly with $\sigma_Z^2$ in the $^{208}$Pb (7.6 MeV/A) + $^{208}$Pb reaction than in the $^{208}$Pb (7.5 MeV/A) + $^{238}$U and $^{238}$U (7.4 MeV/A) + $^{238}$U reactions. In other words, at the same TKEL, $\sigma_Z^2$ is larger in reactions with $^{238}$U than with $^{208}$Pb. The single-particle level density near the Fermi surface in $^{238}$U is also larger than in $^{208}$Pb.

Now consider the influence of the scaling of a level density on the occupation numbers of the single-particle states in the interacting nuclei. In Figs. 3-6, we shown the occupation numbers of neutron and proton single-particle states calculated with the experimentally established (Figs. 3a-6a) and compressed (Figs. 3b-6b) single-particle schemes of Ca while the single-particle scheme of $^{248}$Cm was not changed (Figs. 3c-6c). It can be clearly seen that with an increase in the single-particle level density near the Fermi surface, the transitional region from the occupied to the unoccupied states becomes narrower. This means that the effective temperature characterizing the single-particle occupation numbers in PLF is smaller for the larger level density if the reaction conditions, including the bombarding energy, are the same. For clarity, we have shown also the results of the approximate description of the calculated occupation numbers by the smooth Fermi distribution function with temperature fixed to get a better fit (Figs. 3a-6a). A decrease in the effective temperature characterizing the nucleon occupation numbers in the reaction products with an increase in the single-particle level density near the Fermi surface is just in correspondence with the results demonstrated in Figs. 1-2. The calculations are done for two projectile–target combinations, $^{40,48}$Ca + $^{248}$Cm. In these cases, the projectiles differ by the positions of the chemical potential. Note that the lowest single-particle levels in $^{248}$Cm were not included in the calculations because of the small changes of their occupation numbers. They are not presented in Figs. 3c-6c. Thus, a density of the single-particle levels near the Fermi surface plays a crucial role in a generation of the excitation energy of nuclei.

Closing this section consider some other effects of the shell structure. It is clear that peculiarities of shell structure depend on the neutron numbers. For example, the proton separation energy in $^{40}$Ca and $^{48}$Ca are differed significantly, 8.329 MeV and 15.807 MeV, respectively. To see this effect it is interesting to compare of the values of $R^{P/T}$ presented in Figs. 1a and 2a for $^{40}$Ca +$^{248}$Cm and $^{48}$Ca +$^{248}$Cm reactions. The additional neutrons in $^{48}$Ca lead to an increase of the ratio $R^{P/T}$ for a given value of the total excitation energy. It correlates with the result obtained in [14] that neutrons

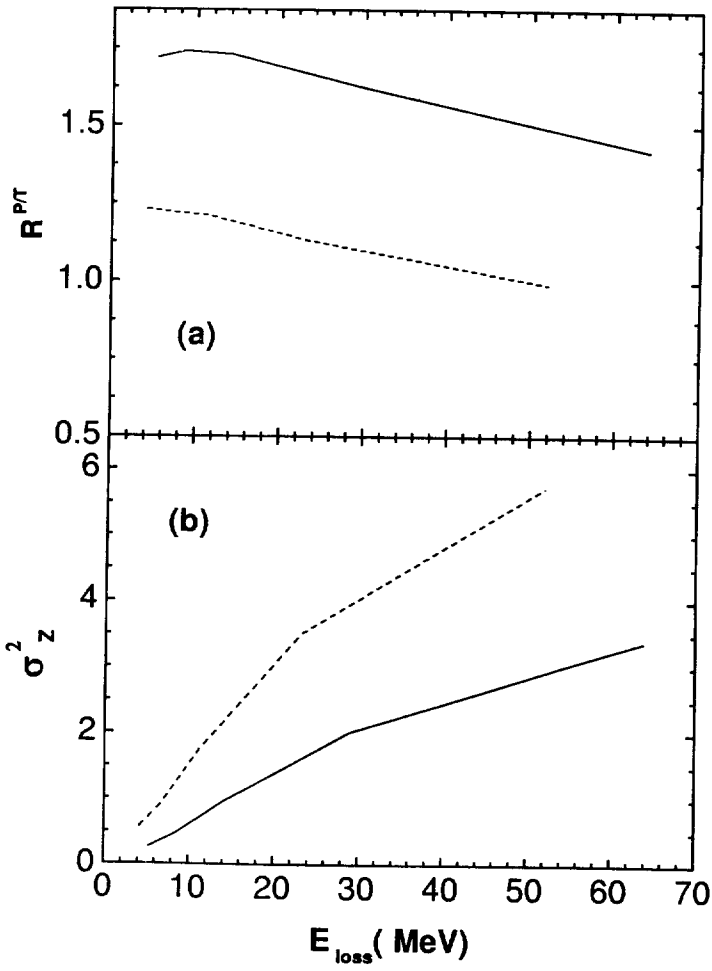


Figure 1: The dependences of the ratio $R^{P/T}$ (a) and the charge variance $\sigma_Z^2$ (b) on $E_{loss}$ for the $^{40}$Ca + $^{248}$Cm reaction, calculated with realistic single-particle schemes (solid curve) and with the single-particle scheme of the light fragment whose single-particle level density near the Fermi surface is doubled (dashed curve). Nucleon separation energies are the same in both cases.

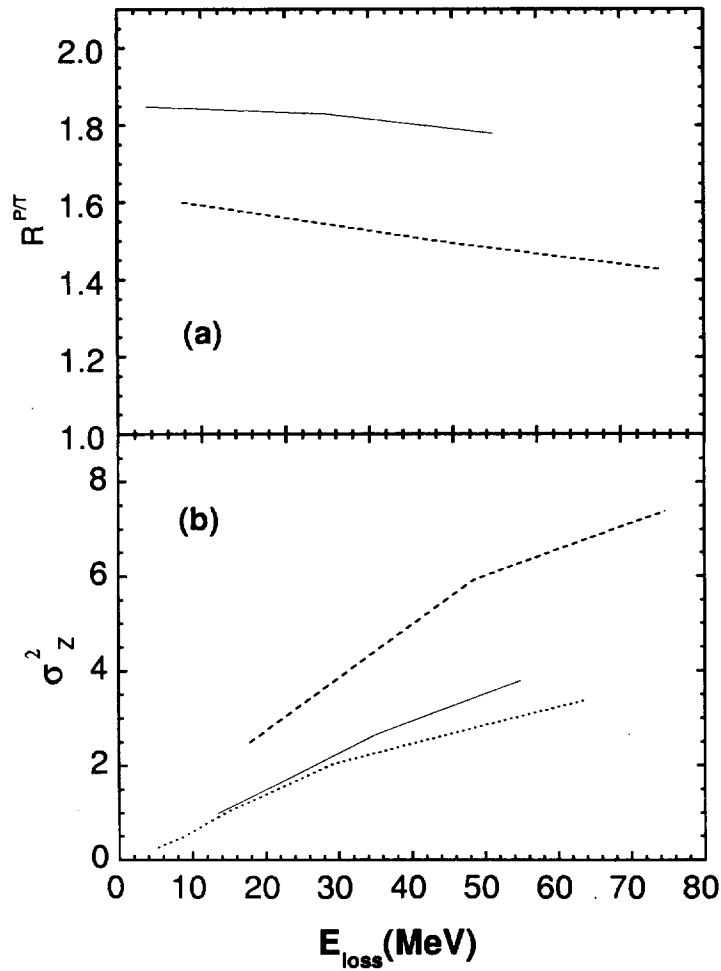


Figure 2: The dependences of the ratio $R^{P/T}$ (a) and the charge variance $\sigma_Z^2$ (b) on $E_{loss}$ for the $^{48}$Ca + $^{248}$Cm reaction, calculated with realistic single-particle schemes (solid curve) and with the single-particle scheme of the light fragment whose single-particle level density near the Fermi surface is doubled (dashed curve). Nucleon separation energies are the same in both cases. For comparison the dependence of the charge variance $\sigma_Z^2$ on $E_{loss}$ for the $^{40}$Ca + $^{248}$Cm reaction, calculated with realistic single-particle schemes (dotted curve), is presented.

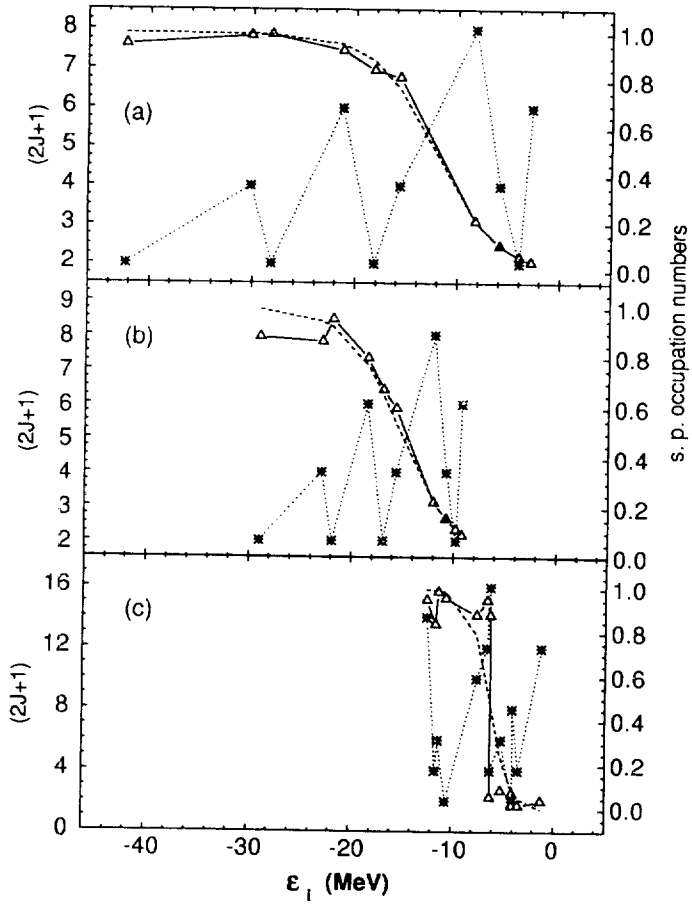


Figure 3: The calculated dynamical (solid curve with triangles) occupation numbers as functions of the neutron single-particle energies in the light fragment for the $^{40}$Ca+$^{248}$Cm deep inelastic collision. The results are obtained with the realistic (a) and compressed (b) the single-particle scheme of $^{40}$Ca while the single-particle scheme of $^{248}$Cm (c) was not changed. Approximate description of the occupation numbers by the Fermi distribution function with temperature is given by the dashed curve with stars. For these quantities, the right ordinate axis is used. For completeness the degeneracies of the single-particle levels are shown by dotted curves with stars (left ordinate axis).

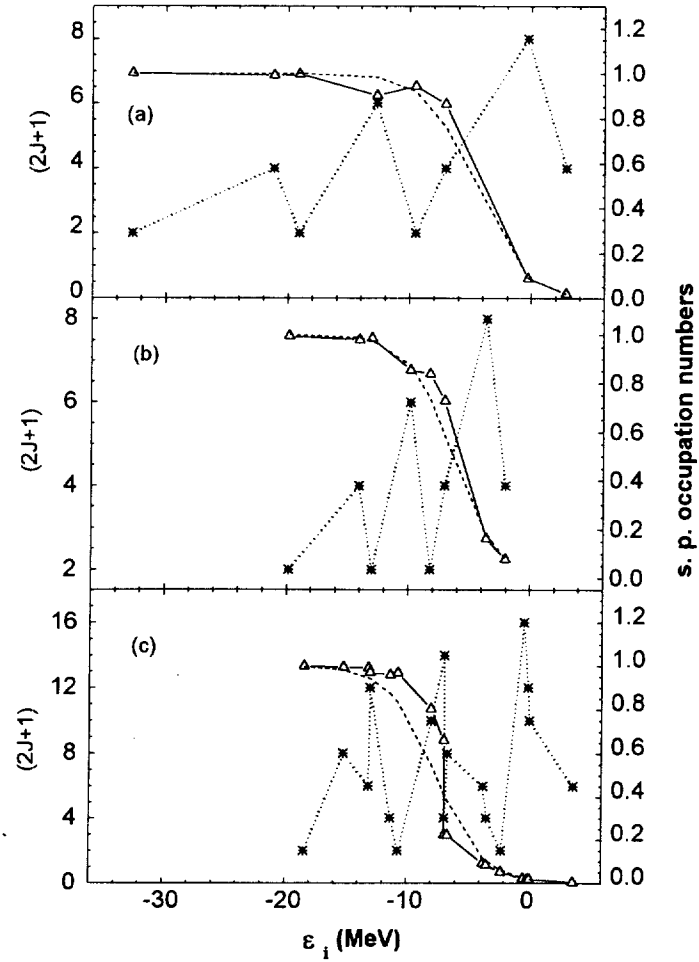


Figure 4: The same as in Fig. 3, but for the proton subsystem in the $^{40}$Ca+$^{248}$Cm reaction.

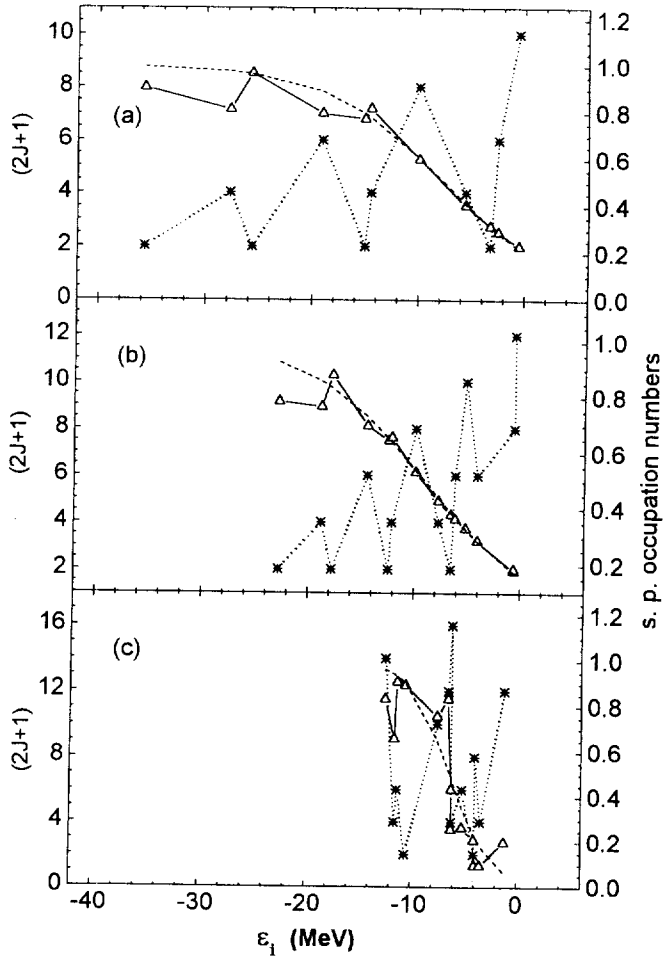


Figure 5: The same as in Fig. 3, but for the neutron subsystem in the $^{48}$Ca $+^{248}$Cm reaction.

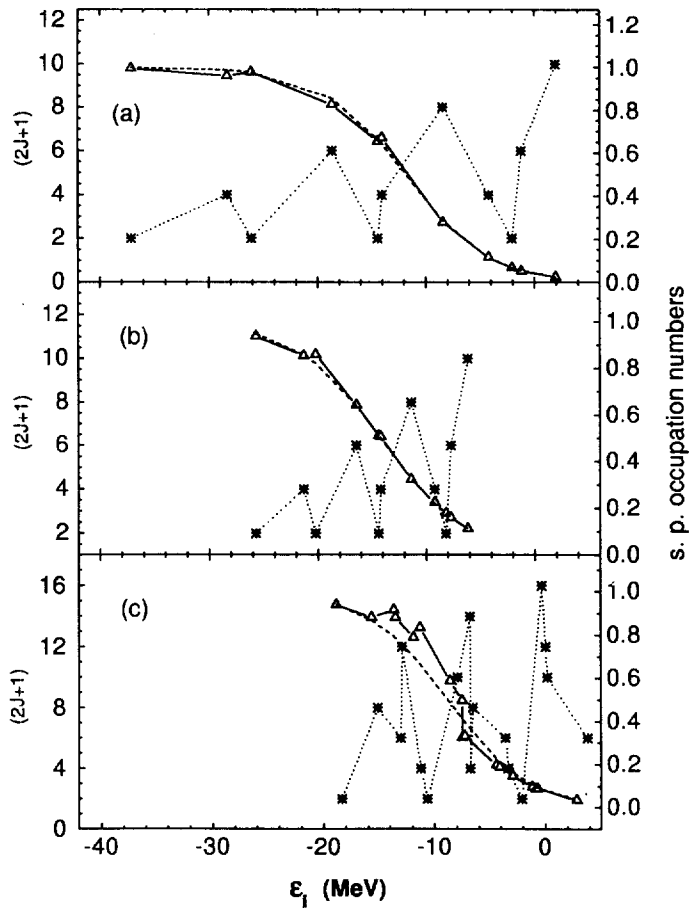


Figure 6: The same as in Fig. 3, but for the proton subsystem in the $^{48}$Ca $+^{248}$Cm reaction.

get more excitation energy than protons. Therefore, an increase of a number of neutrons in a projectile leads to an increase of the ratio $R^{P/T}$.

Another effect of an increase of a neutron number of projectile is seen in a correlation between the charge number variance, $\sigma_Z^2$, and TKEL (Fig. 2b). The curve describing dependence of $\sigma_Z^2$ on TKEL for reaction with $^{40}$Ca is lower than the curve for $^{48}$Ca + $^{248}$Cm reaction at the large TKEL. This result is in a qualitative agreement with the experimental data obtained for the reactions under consideration [17]. This effect can be explained by a difference in the proton separation energies of $^{40}$Ca and $^{48}$Ca. The proton separation energy for $^{48}$Ca ($S_P = 15.807 MeV$) is larger than for $^{40}$Ca ($S_P =$ 8.329 MeV). It means that $^{48}$Ca has more bound states of protons than $^{40}$Ca. So, during deep inelastic collisions the $^{48}$Ca can exchange by a larger number of protons with the target nucleus $^{248}$Cm than $^{40}$Ca. The similar results was observed in reactions with $^{248}$Cm as a target and $1.1 E_{Coul.}$ $^{48}$Ca and $^{40}$Ca as projectiles (Fig. 10. in [17]).

# 4 Conclusion

We have investigated the influence of the single-particle level density of the PLF near the Fermi surface on the ratio of the excitation energies of the light and heavy fragments in DIC. It is shown that a two-fold increasing the single-particle level density of the PLF (the single-particle level scheme of the TLF remains unchanged) decreases the ratio of the excitation energies of the light to heavy fragments by approximately 1.5 times. Since light fragments have smaller single-particle level densities near the Fermi surface than the heavy ones, we consider this result as an indication of the possible reason for the well-known experimental fact that the projectile-to-target excitation energy ratio is significantly larger than the ratio of their masses, as is expected according to thermodynamical arguments. It is shown also that the difference in nucleon separation energies of $^{40}$Ca and $^{48}$Ca effects on the ratio of the excitation energies of projectile- and target-like fragments, $R^{P/T}$, and the correlation between the charge number variance, $\sigma_Z^2$, and TKEL.

The authors (G.G.A., R.V.J., and A.K.N.) thank the Russian Foundation of Basic Research (Grants No. 97-02-16030 and No. 96-15-96729) for the financial support.

# References

[1] Schröder, W.U. and Huizenga, J.R.: Treatise on Heavy-Ion Science: In:

Bromley, D.A. (ed.), Vol.2, New York: Plenum Press 1984, p.115.
[2] Toke, J., Schröder, W.U.: Annu. Rev. Nucl. Part. **42**, 401 (1992).
[3] Randrup, J.: Nucl. Phys. **A307**, 319 (1978); **A327**, 490 (1979).
[4] Ayik, S., Nörenberg W.: Z. Phys. A - Atomic Nuclei, **309**, 121 (1982).
[5] Niita, K., Nörenberg, W., W., Wang, S.J.: Z. Phys. A - Atomic Nuclei, **326**, 69 (1987).
[6] Z. He, P. Rozmej, J. Wu and W. Nörenberg, Nucl.Phys. **A473**, 342 (1987).
[7] H. J. Krappe, Nucl. Phys. **A505**, 417 (1989).
[8] M. Dakowski, P. Doll, A. Gobbi, U. Lynen, A. Olmi, G. Rudolf, H. Sann, and R. Bock, *Proc. Int. Symp. on Continuum Spectra*, held in San Antonio, Texas, December, 1979 (T. Tamura, J.B. Natowitz, and D.H. Youngblood, eds.), Harwood Academic Publishers CHUP, London, New York (1980), Vol. 2, p. 1.
[9] M. Dakowski, P. Doll, A. Gobbi, G. Rudolf, H. Sann, R. Bock, U. Lynen, and A. Olmi, Phys. Lett. **90B**, 379 (1980).
[10] A. Gobbi, Nucl. Phys. **A354**, 337C (1981).
[11] M. Dakowski, A. Gobbi, and W. Nörenberg, Nucl. Phys. **A378**, 189 (1982).
[12] G.G. Adamian, R.V. Jolos, and A.K. Nasirov, Z. Phys. **A347**, 203 (1994).
[13] G.G. Adamian, N.V. Antonenko, R.V. Jolos, and A.K. Nasirov, Phys. Part. Nucl. **A25**, 583 (1994).
[14] G.G. Adamian, R.V. Jolos, A.I. Muminov, and A.K. Nasirov, Phys. Rev. C**53**, 871 (1996).
[15] G.G. Adamian, R.V. Jolos, and A.K. Nasirov, Sov. J. Nucl. Phys. **55**, 660 (1992).
[16] G.G. Adamian, N.V. Antonenko, R.V. Jolos, and A.K. Nasirov, Nucl. Phys. **A551**, 321 (1993).
[17] A. Türler et al., Phys. Rev. C**46**, 1364 (1992).

Received by Publishing Department
on October 7, 1998.

Джолос Р.В. и др.
Е4-98-281

Влияние оболочечной структуры на диссипацию энергии в столкновениях тяжелых ионов

В микроскопическом подходе анализируется влияние оболочечной структуры на распределение энергии возбуждения между продуктами глубоконеупругих столкновений. Показано, что отношение энергий возбуждения фрагментов определяется плотностями одночастичных уровней протонных и нейтронных подсистем вблизи поверхности Ферми на начальной стадии столкновения. Показано, что оболочечная структура влияет на корреляцию между шириной зарядовых распределений и потерей полной кинетической энергии. Расчеты выполнены для реакций $^{40,48}Ca + ^{248}Cm$. Полученные результаты указывают на возможную причину концентрации энергии возбуждения в легком фрагменте, наблюдаемой в глубоконеупругих столкновениях в широком диапазоне потерь полной кинетической энергии.

Работа выполнена в Лаборатории теоретической физики им. Н.Н.Боголюбова ОИЯИ.

Препринт Объединенного института ядерных исследований. Дубна, 1998

Jolos R.V. et al.
E4-98-281

Effect of Shell Structure on Energy Dissipation in Heavy-Ion Collisions

The effect of shell structure on the distribution of the excitation energy between fragments of the deep-inelastic collisions is analysed in the microscopic approach. It is shown that the density of the single-particle levels of the proton and neutron subsystems near the Fermi surface determines the ratio between the excitation energies of fragments at the initial stage of the collision. It is shown also that the shell structure strongly influences the correlations between the width of the charge distributions and the total kinetic energy losses. Calculations are performed for the $^{40,48}Ca + ^{248}Cm$ reactions. The results obtained suggest a possible interpretation for the observed concentration of the excitation energy in the light fragment in deep-inelastic collisions for a wide range of the total kinetic energy losses.

The investigation has been performed at the Bogoliubov Laboratory of Theoretical Physics, JINR.

Preprint of the Joint Institute for Nuclear Research. Dubna, 1998

Макет Т.Е.Попеко

Подписано в печать 29.10.98
Формат 60 × 90/16. Офсетная печать. Уч.-изд. листов 1,71
Тираж 370. Заказ 50979. Цена 2 р.

Издательский отдел Объединенного института ядерных исследований
Дубна Московской области